

Dihydroceramide Desaturase Knockdown Impacts Sphingolipids and Apoptosis after Photodamage in Human Head and Neck Squamous Carcinoma Cells

PAUL BREEN¹, NICHOLAS JOSEPH¹, KYLE THOMPSON¹, JACQUELINE M. KRAVEKA⁴,
TATYANA I. GUDZ^{5,6}, LI LI⁴, MEHRDAD RAHMANIYAN⁴, JACEK BIELAWSKI⁷,
JASON S. PIERCE⁷, ERIC VAN BUREN², GAURAV BHATTI³ and DUSKA SEPAROVIC^{1,2}

¹Department of Pharmaceutical Sciences, Eugene Applebaum College of Pharmacy and Health Sciences,

²Karmanos Cancer Institute, and ³Department of Biomedical Engineering,
School of Engineering, Wayne State University, Detroit, MI, U.S.A.;

⁴Department of Pediatrics Division of Hematology-Oncology, ⁵Ralph H. Johnson Veterans Affairs Medical Center,

⁶Department of Neuroscience, and ⁷Department of Biochemistry and Molecular Biology,
Medical University of South Carolina, Charleston, SC, U.S.A.

Abstract. Background: Dihydroceramide desaturase 1 (DES) is the enzyme responsible for converting dihydroceramide into ceramide in the *de novo* sphingolipid biosynthesis pathway. Dihydroceramide can inhibit ceramide channel formation to interfere with apoptosis. We have shown that following ceramide synthase knockdown, photodynamic therapy (PDT), a cancer treatment modality, is associated with decreased levels of ceramides and dihydroceramides in cells that are resistant to apoptosis. Aim: Here we investigated the effect of DES knockdown on the sphingolipid profile and apoptosis in human head and neck squamous carcinoma cells after PDT with the silicon phthalocyanine Pc 4. Materials and Methods: Following siRNA transfection and PDT treatment, quantitative real-time polymerase chain reaction for quantification of DES mRNA, immunoblotting for protein expression, mass spectrometry for sphingolipid analysis, spectrofluorometry for caspase 3-like (DEVDase) activity, flow cytometry for apoptosis detection, and trypan blue assay for cell viability evaluation, were performed. Results: Down-regulation of DES led to a substantial increase in levels of dihydroceramides without affecting ceramide levels. PDT-induced accumulation of individual dihydroceramides and global ceramides was increased by DES knockdown. Concomitantly, mitochondrial depolarization, DEVDase

activation, late-apoptosis and cell death were attenuated by DES knockdown. Early apoptosis, however, was enhanced. Conclusion: Our findings support the following: (i) dihydroceramide reduces pro-apoptotic effects of ceramide; (ii) cells adapt to DES knockdown to become more sensitive to ceramide and early-apoptosis; (iii) DES is a potential molecular target for regulating apoptotic resistance to PDT.

The sphingolipid ceramide can be generated via the *de novo* sphingolipid biosynthesis pathway (Figure 1), in which dihydroceramide desaturase 1 (DES) introduces the 4,5-trans double bond into the sphingoid backbone of dihydroceramide to give rise to ceramide. The *de novo* ceramide production is activated by apoptotic inducers (1). Although originally thought to be inert, dihydroceramide has been implicated in various processes, including autophagy, cell-cycle arrest and apoptosis (2, 3). Dihydroceramide can inhibit ceramide channel formation and has been proposed to have a negative impact on apoptosis (4). DES knockdown-associated accumulation of dihydroceramide results in cell-cycle arrest (5). Fenretinide, an oxidative stress inducer and a chemopreventive agent, is an *in vitro* inhibitor of DES that induces intracellular accumulation of dihydroceramide and apoptosis (5, 6).

We have shown that the *de novo* sphingolipid biosynthesis pathway affects apoptosis after photodynamic therapy (PDT), a cancer treatment modality (7-9). PDT utilizes a light-absorbing photosensitizer, visible light and oxygen to generate reactive oxygen species that can destroy malignant cellular targets by apoptosis (10, 11). Recently we demonstrated that the knockdown of ceramide synthase 1, or 6, is associated with reduction in ceramides and dihydroceramides, resulting in apoptotic resistance to PDT (12, 13). The objective of the present study was to test for the role of DES in PDT-induced

Correspondence to: Duska Separovic, Department of Pharmaceutical Sciences, Eugene Applebaum College of Pharmacy and Health Sciences, Wayne State University, 259 Mack Ave., Detroit, MI 48201, U.S.A. Tel: +13135778065, Fax: +13135772033, e-mail: dseparovic@wayne.edu

Key Words: Apoptosis, ceramide, dihydroceramide desaturase, dihydroceramide, PDT, sphingolipids, UM-SCC-22A cells, HNSCC.

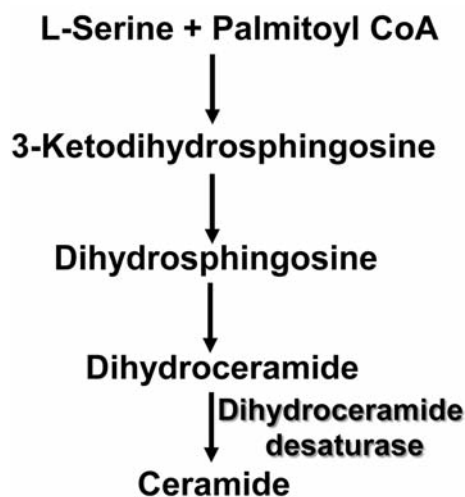


Figure 1. The *de novo* sphingolipid biosynthesis pathway.

sphingolipid production and apoptosis directly. To this end, DES was down-regulated in UM-SCC-22A, a human head and neck squamous carcinoma cell line.

Materials and Methods

Materials. The silicon phthalocyanine Pc 4, $\text{HOSiPcOSi}(\text{CH}_3)_2(\text{CH}_2)_3\text{N}(\text{CH}_3)_2$, was kindly supplied by Dr. Malcolm E. Kenney (Case Western Reserve University, Cleveland, OH, USA). Dulbecco's modified Eagle's medium (DMEM) and serum were from Invitrogen Life Sciences (Grand Island, NY, USA) and Hyclone (Logan, UT, USA), respectively. UM-SCC-22A, a human head and neck squamous carcinoma cell line from hypopharynx (14, 15), was kindly supplied by Dr. Thomas Carey (University of Michigan, Ann Arbor, MI, USA).

Cell culture. UM-SCC-22A cells were grown in DMEM containing 10% fetal bovine serum, 1% non-essential amino acids, 100 U/ml penicillin, and 100 $\mu\text{g}/\text{ml}$ streptomycin. Cells were maintained at 37°C in an incubator with a 5% CO_2 atmosphere, and were treated in the growth medium.

siRNA transfection and PDT treatment. The siRNA targeting the sequence CCU UCA AUG UGG GUU AUC ATT of human DES was from Invitrogen Life Sciences. For control siRNA, AllStars Negative Control siRNA from Qiagen (Valencia, CA, USA) was used. UM-SCC-22A cells were transfected with double-strand siRNAs using Oligofectamine from Invitrogen Life Sciences, according to the manufacturer's instructions. To optimize the concentration of DES, preliminary dose-response experiments (10-40 nM DES) were carried out. As described previously (12), cells (1×10^5 cells/ml) were transfected with 25 nM of each siRNA. Twenty-four hours after transfection, cells were collected and seeded in fresh-growth medium. Following overnight exposure to Pc 4 (250 and 500 nM), cells were irradiated with red light (2 mW/cm^2 ; $\lambda_{\text{max}} \sim 670$ nm) using a light-emitting diode array (EFOS; Mississauga, ONT, Canada) at a fluence of 200 mJ/cm^2 at room temperature. Following PDT, cells were incubated

at 37°C for 2 or 24 h, collected on ice and processed for various analyses. For mass spectrometric analysis, cells were washed twice with cold phosphate-buffered saline, sonicated in a mixture of ethyl acetate/methanol (1:1, v/v), dried under nitrogen, and shipped overnight on dry ice to the Lipidomics Shared Resource (Medical University of South Carolina, Charleston, SC, USA) for further processing.

Sphingolipid analysis by quantitative high-performance liquid chromatography (HPLC)/mass spectrometry (MS). Following extraction, sphingolipids were separated by HPLC, introduced to an electrospray ionization source and then analyzed by double-MS using a TSQ Quantum Access mass spectrometer from ThermoFisher Scientific (Waltham, MA, USA), as described previously (16).

RNA extraction and quantitative real-time polymerase chain reaction (PCR). Total RNA isolation was performed with the RNeasy[®] Mini Kit (Qiagen) according to the manufacturer's instructions. cDNA was synthesized from 1 μg of the total RNA using iScript[™] cDNA Synthesis Kit (Bio-Rad, Hercules, CA, USA). The concentration and quality of total RNA preparations were evaluated spectrophotometrically. PCR was performed on a Bio-Rad iCycler detection system using Bio-Rad SsoFast Probes Supermix[™] and TaqMan[®] Gene Expression Assays (Life Technologies Corporation, Carlsbad, CA, USA) primer/probe sets for *DES* and the ribosomal protein L13A (RPL13A). Initial steps of PCR were 30 s at 85°C, followed by 40 cycles consisting of a 5 s at 95°C, followed by 10 s at 60°C. Determination of the relative quantities of *DES* mRNA against the internal control housekeeping gene *rpl13a*, was performed by following a ΔCT method (17).

Immunoblotting. Following PDT, cells were collected, lysed in reducing Laemmli buffer, boiled and then subjected to sodium dodecyl sulfate-polyacrylamide gel electrophoresis (SDS-PAGE), and western immunoblotting, as reported previously (7, 18). Equal protein loading was confirmed using antibody against heat shock protein 90 (HSP-90). Antibody against DES (MLD 3906) was synthesized by Dr. Gordon N. Gill (University of California, San Diego, CA, USA). Mouse monoclonal anti-HSP-90 was from BD Biosciences (San Diego, CA, USA). Following visualization of blots using the ECL Plus chemifluorescence kit and STORM 860 imaging system (GE Healthcare, Piscataway, NJ, USA), they were quantified by ImageQuant 5.2 (GE Healthcare).

Caspase 3-like (DEVDase) activity assay. As described previously (12), following PDT, cell harvesting and cell lysis, DEVDase activity was measured using a fluorogenic derivative of the tetrapeptide substrate Asp-Glu-Val-Asp [Ac-DEVD-AMC (7-amino-4-methylcoumarin)] from Enzo Life Sciences (Farmingdale, NY, USA), and an F-2500 spectrofluorometer (Hitachi; Dallas, TX, USA) (380 nm excitation, 460 nm emission).

Mitochondrial membrane depolarization measurement. The lipophilic cationic dye JC-1 (5,5',6,6'-tetrachloro-1,1',3,3'-tetraethylbenzimidazolylcarbocyanine iodide) from BD Biosciences (San Diego, CA, USA) was used to determine mitochondrial membrane potential by flow cytometry, as we have described previously (8, 12, 19). Following PDT, cells were harvested and processed for flow cytometry according to the manufacturer's instructions (BD Biosciences). A BD LSR II flow cytometer was used for analysis (BD Biosciences).

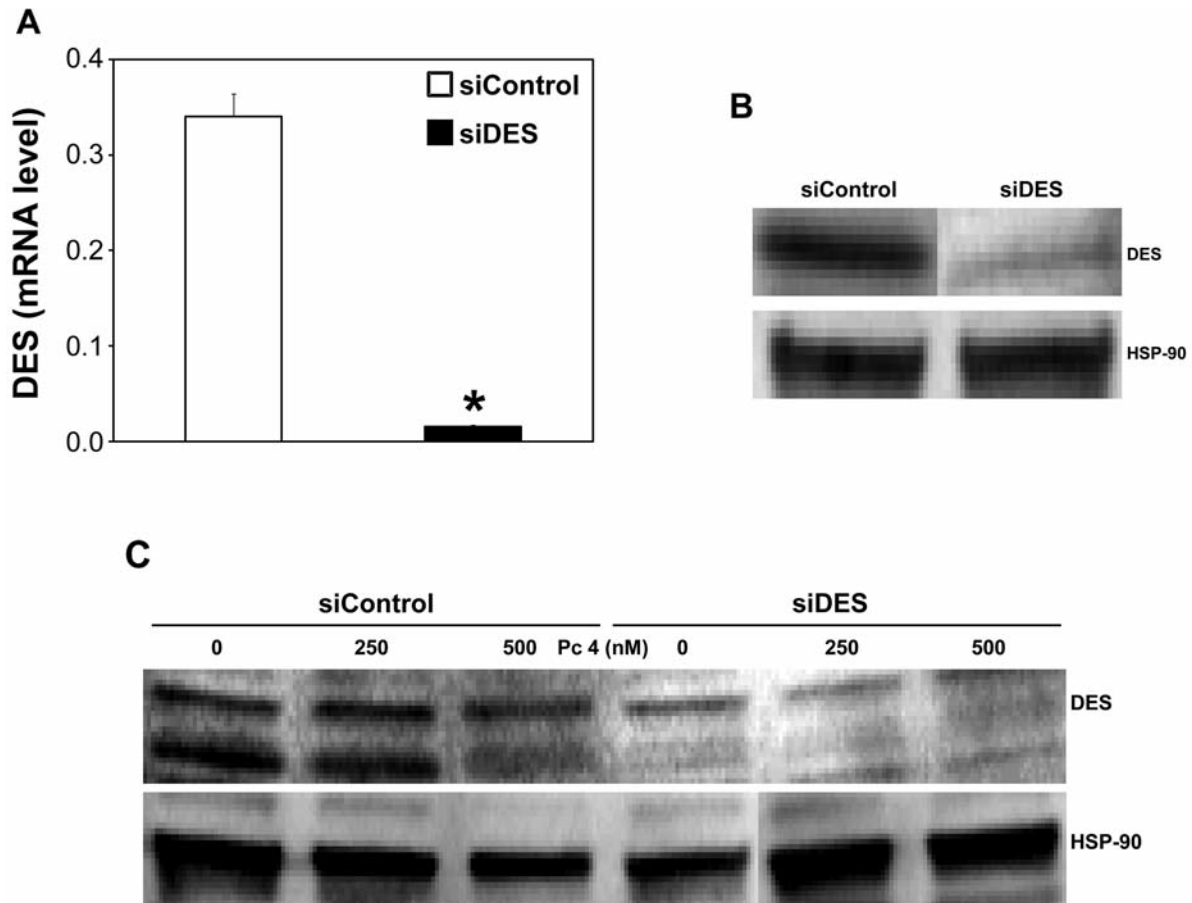


Figure 2. Dihydroceramide desaturase 1 (DES) is down-regulated by DES knockdown. UM-SCC-22A cells were transfected with siRNA targeted against non-targeted control (siControl; 25 nM) or DES (siDES; 25 nM). Twenty-four hours after transfection, cells were collected, seeded in fresh growth medium, incubated at 37°C for an additional 24 h, collected, and processed for real-time-polymerase chain reaction (PCR) (A) and sodium dodecyl sulfate-polyacrylamide gel electrophoresis (SDS-PAGE)/western immunoblotting (B and C). A: DES mRNA levels are expressed in arbitrary units. The data are shown as the mean±SEM, * $p \leq 0.05$, $n = 5-6$. B: DES knockdown was confirmed in two independent experiments. C: Following overnight exposure to Pc 4 (250 and 500 nM), cells were irradiated with red light, incubated at 37°C for 2 h, collected and processed for SDS-PAGE/western immunoblotting. B and C: Equal protein loading was verified using anti-heat shock protein 90 (HSP-90).

Trypan blue dye exclusion assay. After PDT, cells were harvested, re-suspended in cell growth medium and diluted 1:1 with 0.4% trypan blue stain from Sigma-Aldrich (St. Louis, MO, USA). Stained and unstained cells were counted using a hemocytometer. Trypan blue-positive cells were designated as dead cells.

Statistical analysis. For MS data, a linear model was used to determine the effects of cell line and PDT (independent variables) on the concentration of sphingolipids (dependent variable). The nominal p -values obtained from the model were adjusted across all individual sphingolipids to control the false-discovery rate at 5%. For effects on global ceramides and dihydroceramides, a one-sample t -test was used on individual log₂ ratios (PDT/control) within the family of ceramides or dihydroceramides, in order to determine whether the ratios were different from unity. All analyses were performed using an R statistical language. For all other data the average value and the standard error were calculated for at least

$n = 3$. Data were analyzed for statistically significant differences ($p \leq 0.05$) between groups using a t -test of unequal variance.

Results

DES was down-regulated at-rest and after PDT. To verify down-regulation of DES in siDES-transfected cells (siDES cells), DES mRNA and protein expression were determined. DES mRNA was reduced by >90% 48 h after transfection (Figure 2A) and the effect was maintained after 72 h (not shown). DES protein levels were reduced by 48% after DES knockdown (Figure 2B; quantifiable data not shown).

We next examined the effect of PDT on DES expression in both cell types. As shown in Figure 2C, DES was degraded after treatment with 500 nM Pc 4/PDT in siControl-

Table I. Effect of dihydroceramide desaturase 1 (DES) knockdown on resting levels of global sphingolipids.

Global sphingolipids	p-Value	Fold-change [†]
Ceramides	0.17	-1.33
Dihydroceramides	0.00001	+26.64

[†]In siDES-transfected cells relative to that of siControl-transfected cells.

transfected cells (siControl cells). The effect was not apparent at 250 nM Pc 4/PDT. In untreated siDES cells, DES was down-regulated. No further effect of PDT on the protein expression was detected.

Resting levels of global dihydroceramides were substantially raised by DES knockdown. At rest, DES silencing markedly increased global levels of dihydroceramides without affecting the levels of ceramides (Table I). Individually, the resting levels of C14-, C16-, C22-, C22:1-, C24-, C24:1-, C26-, and C26:1-dihydroceramide were significantly increased by DES knockdown (Table II). The resting levels of individual ceramides were not significantly affected by DES knockdown (not shown). The accumulation of dihydrosphingosine, an intermediate in the *de novo* biosynthesis pathway was significantly increased after the knockdown (data not shown). Overall, increases in global and individual dihydroceramides further verifies DES knockdown.

The effect of DES knockdown on the sphingolipid profile after PDT. We then explored the effect of DES silencing on the sphingolipid profile in siControl and siDES cells at 2 h post-PDT (Table III). Globally, ceramides were increased in siControl cells after both PDT doses. In siDES cells, a significant increase in global ceramides was observed only after the higher PDT dose, and that increase was higher than in siControl cells ($p < 0.011$). Global levels of dihydroceramides were increased in both cell types after both PDT doses. The responses were generally lower in siDES cells than in siControl cells due to higher baseline levels of dihydroceramides. Thus, DES knockdown is associated with increases in global dihydroceramides and, at the higher PDT dose, global ceramide levels.

Among individual ceramides that were significantly increased after PDT in both cell types are: C14-, C16-, C18-, and C18:1-ceramide (Table IV). There were no differences between the two cell types in individual ceramide responses to PDT. Individual dihydroceramides that were significantly increased post-PDT in both cell types are: C14-, C16-, C18-, C18:1-, C20:1-, and C22:1-dihydroceramide (Table V). PDT-induced levels of C14-, C16-, C18-, C22:1-, and C24:1-dihydroceramide were significantly higher ($p < 0.05$) in

Table II. Dihydroceramide desaturase 1 (DES) knockdown increases resting levels of individual ceramides.

Dihydroceramide	FDR*	Fold-change [†]
C14-	0.0002	14.15
C16-	0.0004	10.36
C22-	0.03	62.50
C22:1-	0.004	80.24
C24-	0.03	146.49
C24:1-	0.003	272.74
C26-	0.03	77.62
C26:1-	0.03	65.39

*Adjusted p-values using the false discovery rate (FDR) adjustment algorithm. Only the levels of dihydroceramides that were significantly higher are shown. [†]In siDES-transfected cells relative to that of siControl-transfected cells.

siControl than in siDES cells. In contrast, the induced accumulation of C20- and C24-dihydroceramide was higher ($p < 0.03$) in siDES-cells than in their control counterparts. In addition, significant increases in dihydrosphingosine and sphingosine were observed after PDT in both cell types (Table VI). Dihydrosphingosine response was greater in siControl cells than in siDES cells.

DES knockdown inhibited PDT-induced DEVDase activation. To assess the requirement for DES in PDT-induced caspase-3 activation, we measured the DEVDase activity at 2 h after PDT in both cell types. We found that DES knockdown led to a 23 and 34% reduction in DEVDase activation, after corresponding PDT doses (Figure 3). These findings are consistent with the idea that DES is involved in PDT-induced activation of DEVDase.

DES knockdown suppressed mitochondrial depolarization after PDT. The loss of mitochondrial membrane potential accompanies PDT-evoked apoptosis (8, 21). We asked whether DES affects apoptosis at the mitochondrial level 24 h after PDT. As shown in Figure 4A, following DES knockdown, mitochondrial depolarization was reduced by 18%, after 250 nM Pc 4/PDT. A similar effect was observed after 500 nM Pc 4/PDT. The data support the notion that mitochondrial depolarization after PDT is DES-dependent.

The effect of DES knockdown on PDT-induced apoptosis. We investigated the role of DES in apoptosis at 24 h after PDT using annexin V and propidium iodide as early- and late-apoptotic markers, respectively. As depicted in Figure 4B, following DES knockdown the appearance of annexin V⁺/propidium iodide⁻ cells was suppressed only after 250 nM

Table III. The effect of photodynamic therapy (PDT) on global sphingolipids in siControl- and siDES-transfected cells.

Cell type	Pc 4 (nM) for PDT	Global ceramides <i>p</i> -Value	Fold-change [†]	Global dihydroceramides <i>p</i> -Value	Fold-change [†]
siControl	250	0.01	1.78	0.00001	12.51
	500	0.01	2.21	0.0001	10.10
siDES	250	0.11	1.73	0.01	4.01
	500	0.00005	3.92*	0.00004	5.68

[†]Post-PDT relative to that in untreated controls. *The increase in global ceramides after PDT was higher in siDES- than in siControl-transfected cells ($p < 0.011$). DES, Dihydroceramide desaturase 1.

Table IV. The effect of photodynamic therapy (PDT) on levels of individual ceramides in siControl- and siDES-transfected cells.

Ceramide	250 nM Pc 4/PDT FDR*	Fold- change [†]	500 nM Pc 4/PDT FDR*	Fold- change [†]
siControl				
C14-			0.007	3.66
C16-	0.005	2.65	0.001	3.62
C18-	0.005	5.50	0.004	4.48
C18:1-	0.005	3.52	0.001	5.30
C20:1-			0.008	6.79
siDES				
C14-	0.014	3.84	0.004	4.93
C16-	0.014	2.09	0.0002	4.88
C18-	0.053	7.32	0.013	12.69
C18:1-	0.009	9.95	0.001	15.46
C20-			0.004	4.18

[†]Post-PDT relative to that in untreated controls. *Adjusted *p*-values using the false discovery rate (FDR) adjustment algorithm. Only the levels of ceramides that were significantly higher are shown. DES, Dihydroceramide desaturase 1.

Pc 4/PDT. In contrast, *DES* knockdown led to enhanced appearance of annexin V⁺/propidium iodide⁻ cells after 500 nM Pc 4/PDT. Furthermore, *DES* knockdown resulted in moderate reduction in the appearance of annexin V⁺/propidium iodide⁺ cells after both PDT doses. These findings suggest that *DES* knockdown has a dual, dose-dependent effect on early apoptosis, by making the cells either more resistant or more sensitive to PDT. *DES* knockdown conferred moderate resistance to late PDT-induced apoptosis. Taken together, these findings support the notion that DES is involved in controlling apoptotic response to PDT.

DES knockdown attenuated PDT-induced cell death. To assess the effect of *DES* knockdown on cell viability at 24 h post-PDT, the trypan blue dye exclusion assay was used. Approximately 80% of trypan blue-positive cells were detected after treatment with both PDT doses (Figure 4C). Their number was only moderately, but significantly, reduced following *DES* knockdown.

Table V. The effect of photodynamic therapy (PDT) on individual dihydroceramides in siControl- and siDES-transfected cells.

Dihydro- ceramide	250 nM Pc 4/PDT FDR*	Fold- change [†]	500 nM Pc 4/PDT FDR*	Fold- change [†]
siControl				
C14-	2.9E-08	34.89**	2.6E-08	32.47**
C16-	3.8E-08	27.38**	2.6E-08	31.64**
C18-	0.00006	125.49**	0.00009	98.77**
C18:1-	0.044	9.21	0.026	12.06
C20-			0.21	2.16
C20:1-			0.040	17.74
C22-	0.054	10.03		
C22:1-	0.0002	46.08**	0.001	19.25**
C24-			0.99	1.02
C24:1-	0.039	8.39	0.019	11.74**
C26:1-	0.054	11.86		
siDES				
C14-	0.002	6.61	0.002	7.81
C16-	0.00005	5.81	0.00001	8.12
C18-	0.001	51.81	0.002	37.75
C18:1-	0.03	11.29		
C20-	0.01	11.80	0.01	13.39***
C20:1-	0.01	15.14	0.01	11.42
C22:1-	0.001	6.40	0.07	1.98
C24-			0.14	4.07***
C24:1-			0.14	2.06

[†]Post-PDT relative to that in untreated controls. Only the data that are of statistical relevance are shown. *Adjusted *p*-values using the false discovery rate (FDR) adjustment algorithm. **Higher in siControl- than in siDES-transfected cells. ***Higher in siDES-transfected cells than in their control counter parts. DES, Dihydroceramide desaturase 1.

Discussion

The present study shows that by knocking down *DES*, levels of dihydroceramides are substantially elevated without any significant changes in ceramides at-rest. Despite the reduction in DES, there are still significant increases in ceramides following PDT. Specifically, at 500 nM Pc 4/PDT levels of global ceramides are higher in siDES cells than in their control counterparts. This increase correlates with enhanced early-apoptosis. However, the cells remain resistant

Table VI. The effect of photodynamic therapy (PDT) on other sphingolipids in siControl- and siDES-transfected cells.

	250 nM Pc 4 /PDT FDR*	Fold-change [†]	500 nM Pc 4 /PDT FDR*	Fold-change [†]
siControl				
Dihydrosphingosine	0.0001	6.86**	1.5E-06	17.01**
Sphingosine	0.002	3.45	6.3E-07	41.07
siDES				
Dihydrosphingosine	4.0E-05	4.18	1.1E-06	8.13
Sphingosine	0.001	3.85	9.0E-07	44.26

[†]Post-PDT relative to that in untreated controls. *Adjusted *p*-values using the false discovery rate (FDR) adjustment algorithm. **Higher in siControl-transfected cells. DES, Dihydroceramide desaturase 1.

to mitochondrial depolarization, DEVDase activation and late apoptosis. This is likely due to alteration in dihydroceramide/ceramide balance after *DES* knockdown. Besides increases in global ceramides, the levels of C20- and C24-dihydroceramide are greater in siDES cells. PDT-induced increases in individual dihydroceramides in siDES cells counteract pro-apoptotic effects of ceramide. Our data support the idea that DES affects the dihydroceramide/ceramide balance, and consequently, apoptotic responsiveness to PDT. Similarly, DES-dependent shift in dihydroceramide/ceramide balance has been proposed to control cell growth and death in hypoxia/reoxygenation (22).

The following scenario might be proposed as to how the dihydroceramide/ceramide shift regulates PDT-induced apoptosis: pro-apoptotic ceramide forms channels in the outer mitochondrial membrane and, with activated Bax, synergizes to induce mitochondrial depolarization (23, 24). Elevated dihydroceramides prevent ceramide channel formation (4) to counteract pro-apoptotic effects of ceramide. Since Bax is required for mitochondrial apoptotic pathway after PDT (25), we propose that PDT-induced enhanced levels of C20- and C24-dihydroceramide in siDES cells lead to inhibition of ceramide channel formation to hinder mitochondrial depolarization, with subsequent inhibition of DEVDase activation. Apparently, early apoptosis-related phosphatidylserine translocation to the outer leaflet of the plasma membrane is less impacted by dihydroceramide and more responsive to elevated ceramide levels.

PDT-induced enhanced increases in global ceramide in siDES cells are likely due to incomplete *DES* knockdown, allowing for *de novo* ceramide to be formed. The activation of the salvage pathway can be eliminated based on the following: our current findings show that PDT-induced increases in sphingosine are not different between the two cell types, and therefore, are not *DES* knockdown-dependent; our previous studies showed that acid sphingomyelinase (26) and ceramidase (unpublished observations) are inhibited by PDT.

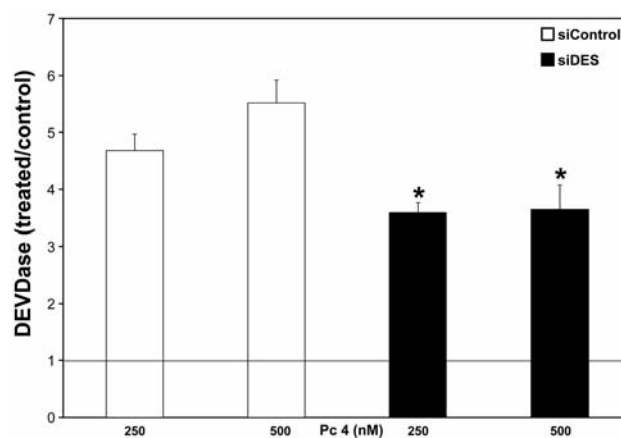


Figure 3. Dihydroceramide desaturase 1 (*DES*) knockdown suppressed caspase 3-like (*DEVDase*) activation after photodynamic therapy (PDT). Following 2-h incubations post-PDT, cells were collected, lysed, and *DEVDase* activity was measured using Ac-*DEVD*-AMC as the fluorogenic substrate. The data are expressed as ratios of PDT-treated versus untreated controls and are shown as the mean±SEM, n=3-7. **DES* knockdown suppresses PDT-induced *DEVDase* activation (*p*≤0.05).

Oxidative stress has been shown to inhibit *DES* without affecting *DES* protein levels (27). In contrast, our current study shows degradation of *DES* post-treatment with 500 nM Pc 4/PDT in siControl cells. PDT-induced destruction of *DES* did not further increase accumulation of global dihydroceramides. The loss of *DES* is likely due to PDT-induced oxidative stress, as our previous studies have shown (9).

Our novel findings have the following implications: (i) dihydroceramide acts as a modifying factor, reducing pro-apoptotic effects of ceramide; (ii) cells adapt to *DES* knockdown to become more sensitive to ceramide and early apoptosis; (iii) *DES* is a potential molecular target for regulating apoptotic resistance to PDT.

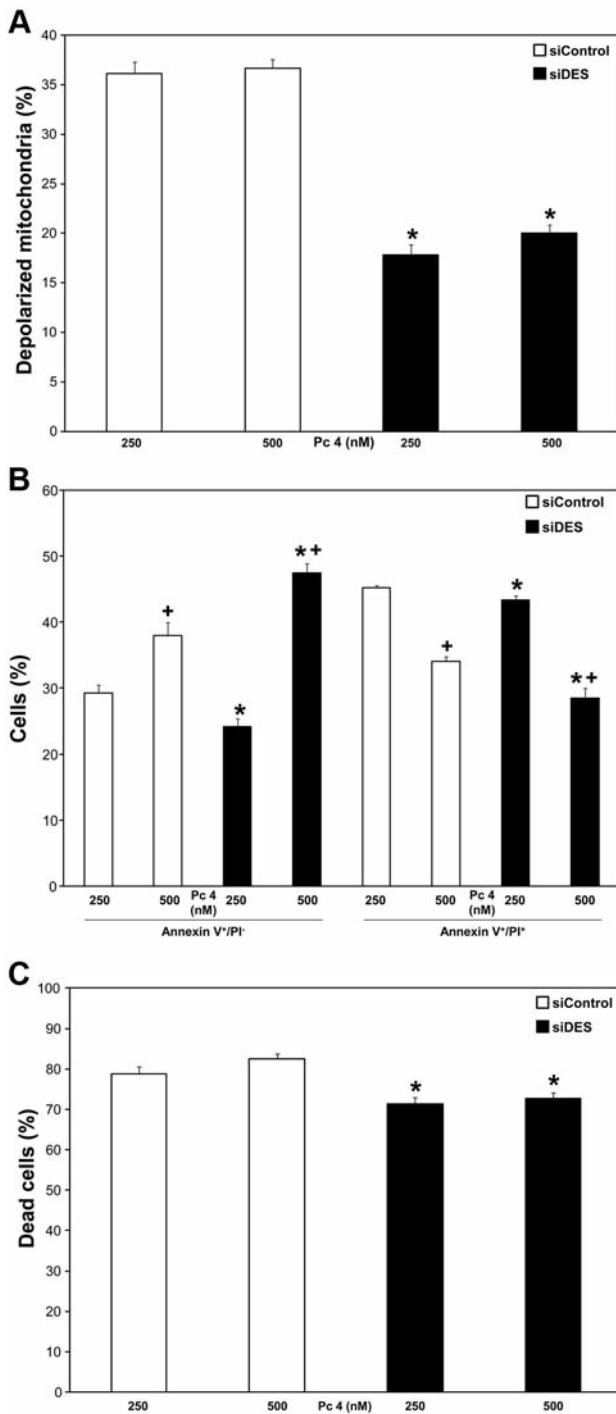


Figure 4. Dihydroceramide desaturase 1 (DES) knockdown suppressed mitochondrial depolarization, apoptosis and cell death after photodynamic therapy (PDT). Following 24-h incubation post-PDT, cells were collected and processed for flow cytometry (A, B), or stained with trypan blue and counted (C). JC-1 and annexin V/propidium iodide (PI) staining were used to detect mitochondrial membrane potential (A) and apoptosis (B), respectively. The data are shown as the mean \pm SEM, n=3-7. The significance ($p\leq 0.05$) is indicated as follows: *DES knockdown affects PDT-induced, mitochondrial depolarization, apoptosis, or cell death; +apoptosis is different between the two PDT doses.

Acknowledgements

This work was supported by: U.S. Public Health Service Grants from the National Institutes of Health R01 CA77475 (DS), and P20-RR17677 (JMK); grants from the Rally Foundation for Childhood Cancer Research, Hyundai Hope on Wheels, Monica Kreber Golf Tournament, and Chase after a Cure Foundation (JMK); the Veterans Administration Merit Awards from RR&D and BLRD programs (TIG). The MS-related work was performed by the Lipidomics Shared Resource (Medical University of South Carolina), supported by NCI grants: IPO1CA097132 and P30 CA 138313 and NIH/NCRR SC COBRE Grant P20 RR017677. Laboratory space for the Lipidomics Shared Resource was supported by the NIH, grant C06 RR018823 from the Extramural Research Facilities Program of the National Center for Research Resources.

References

- Bartke N and Hannun YA: Bioactive sphingolipids: Metabolism and function. *J Lipid Res* 50(Suppl): S91-96, 2009.
- Fabrias G, Munoz-Olaya J, Cingolani F, Signorelli P, Casas J, Gagliostro V and Ghidoni R: Dihydroceramide desaturase and dihydrosphingolipids: Debutant players in the sphingolipid arena. *Prog Lipid Res* 51: 82-94, 2012.
- Zheng W, Kollmeyer J, Symolon H, Momin A, Munter E, Wang E, Kelly S, Allegood JC, Liu Y, Peng Q, Ramaraju H, Sullards MC, Cabot M and Merrill AH Jr.: Ceramides and other bioactive sphingolipid backbones in health and disease: Lipidomic analysis, metabolism and roles in membrane structure, dynamics, signaling and autophagy. *Biochim Biophys Acta* 1758: 1864-1884, 2006.
- Stiban J, Fistere D and Colombini M: Dihydroceramide hinders ceramide channel formation: Implications on apoptosis. *Apoptosis* 11: 773-780, 2006.
- Kraveka JM, Li L, Szulc ZM, Bielawski J, Ogretmen B, Hannun YA, Obeid LM and Bielawska A: Involvement of dihydroceramide desaturase in cell cycle progression in human neuroblastoma cells. *J Biol Chem* 282: 16718-16728, 2007.
- Rahmaniyan M, Curley RW, Jr, Obeid LM, Hannun YA and Kraveka JM: Identification of dihydroceramide desaturase as a direct *in vitro* target for fenretinide. *J Biol Chem* 286: 24754-24764, 2011.
- Dolgachev V, Farooqui MS, Kulaeva OI, Tainsky MA, Nagy B, Hanada K and Separovic D: De novo ceramide accumulation due to inhibition of its conversion to complex sphingolipids in apoptotic photosensitized cells. *J Biol Chem* 279: 23238-23249, 2004.
- Dolgachev V, Nagy B, Taffe B, Hanada K and Separovic D: Reactive oxygen species generation is independent of *de novo* sphingolipids in apoptotic photosensitized cells. *Exp Cell Res* 288: 425-436, 2003.
- Wispriyono B, Schmelz E, Pelayo H, Hanada K and Separovic D: A role for the *de novo* sphingolipids in apoptosis of photosensitized cells. *Exp Cell Res* 279: 153-165, 2002.
- Agostinis P, Berg K, Cengel KA, Foster TH, Girotti AW, Gollnick SO, Hahn SM, Hamblin MR, Juzeniene A, Kessel D, Korblick M, Moan J, Mroz P, Nowis D, Piette J, Wilson BC and Golab J: Photodynamic therapy of cancer: An update. *CA Cancer J Clin* 61: 250-281, 2011.
- Oleinick N, Morris R and Nieminen A-L. Photodynamic Therapy-Induced Apoptosis. *In: Apoptosis, Senescence and Cancer*. Gewirtz DA, Holt SE and Grant S (eds.). Totowa: Humana Press Inc. pp. 557-578, 2007.

- 12 Separovic D, Breen P, Joseph N, Bielawski J, Pierce JS, Van Buren E and Gudz TI: Ceramide synthase 6 knockdown suppresses apoptosis after photodynamic therapy in human head and neck squamous carcinoma cells. *Anticancer Res* 32: 753-760, 2012.
- 13 Separovic D, Breen P, Joseph N, Bielawski J, Pierce JS, Van Buren E and Gudz TI: siRNA-mediated down-regulation of ceramide synthase 1 leads to apoptotic resistance in human head and neck squamous carcinoma cells after photodynamic therapy. *Anticancer Res* 32: 2479-2485, 2012.
- 14 Brenner JC, Graham MP, Kumar B, Saunders LM, Kupfer R, Lyons RH, Bradford CR and Carey TE: Genotyping of 73 UM-SCC head and neck squamous cell carcinoma cell lines. *Head Neck* 32: 417-426, 2010.
- 15 Zhu Z, Xu X, Yu Y, Graham M, Prince ME, Carey TE and Sun D: Silencing heat-shock protein 27 decreases metastatic behavior of human head and neck squamous cell cancer cells *in vitro*. *Mol Pharm* 7: 1283-1290, 2010.
- 16 Separovic D, Semaan L, Tarca AL, Awad Maitah MY, Hanada K, Bielawski J, Villani M and Luberto C: Suppression of sphingomyelin synthase 1 by small interference RNA is associated with enhanced ceramide production and apoptosis after photodamage. *Exp Cell Res* 314: 1860-1868, 2008.
- 17 Pfaffl MW: A new mathematical model for relative quantification in real-time RT-PCR. *Nucleic Acids Res* 29: e45, 2001.
- 18 Separovic D, Kelekar A, Nayak AK, Tarca AL, Hanada K, Pierce JS and Bielawski J: Increased ceramide accumulation correlates with down-regulation of the autophagy protein ATG-7 in MCF-7 cells sensitized to photodamage. *Arch Biochem Biophys* 494: 101-105, 2010.
- 19 Separovic D, Saad ZH, Edwin EA, Bielawski J, Pierce JS, Van Buren E and Bielawska A: C16-ceramide analog combined with Pc 4 photodynamic therapy evokes enhanced total ceramide accumulation, promotion of DEVDase activation in the absence of apoptosis, and augmented overall cell killing. *J Lipids* 2011: 1-9, 2011.
- 20 Separovic D, Mann KJ and Oleinick NL: Association of ceramide accumulation with photodynamic treatment-induced cell death. *Photochem Photobiol* 68: 101-109, 1998.
- 21 Lam M, Oleinick NL and Nieminen AL: Photodynamic therapy-induced apoptosis in epidermoid carcinoma cells. Reactive oxygen species and mitochondrial inner membrane permeabilization. *J Biol Chem* 276: 47379-47386, 2001.
- 22 Devlin CM, Lahm T, Hubbard WC, Van Demark M, Wang KC, Wu X, Bielawska A, Obeid LM, Ivan M and Petrache I: Dihydroceramide-based response to hypoxia. *J Biol Chem* 286: 38069-38078, 2011.
- 23 Ganesan V, Perera MN, Colombini D, Datskovskiy D, Chadha K and Colombini M: Ceramide and activated Bax act synergistically to permeabilize the mitochondrial outer membrane. *Apoptosis* 15: 553-562, 2010.
- 24 Siskind LJ, Kolesnick RN and Colombini M: Ceramide channels increase the permeability of the mitochondrial outer membrane to small proteins. *J Biol Chem* 277: 26796-26803, 2002.
- 25 Chiu SM, Xue LY, Usuda J, Azizuddin K and Oleinick NL: Bax is essential for mitochondrion-mediated apoptosis but not for cell death caused by photodynamic therapy. *Br J Cancer* 89: 1590-1597, 2003.
- 26 Nagy B, Chiu S-M and Separovic D: Fumonisin B1 does not prevent apoptosis in A431 human epidermoid carcinoma cells after photosensitization with phthalocyanine 4. *J Photochem Photobiol B: Biology* 57: 132-141, 2000.
- 27 Idkowiak-Baldys J, Apraiz A, Li L, Rahmaniyan M, Clarke CJ, Kravcka JM, Asumendi A and Hannun YA: Dihydroceramide desaturase activity is modulated by oxidative stress. *Biochem J* 427: 265-274, 2010.

Received November 15, 2012

Revised November 29, 2012

Accepted November 30, 2012